Annals of Nuclear Medicine Vol. 16, No. 5, 303–310, 2002

Technical and analytical advances in pulmonary ventilation SPECT with xenon-133 gas and Tc-99m-Technegas

Kazuyoshi SUGA

Department of Radiology, Yamaguchi University School of Medicine

This paper describes the recent advances in technical and analytical methods in pulmonary ventilation SPECT studies, including a respiratory-gated image acquisition of Technetium-99m (^{99m}Tc)-labeled Technegas SPECT, a fusion image between Technegas SPECT and chest CT images created by a fully automatic image registration algorithm, and a three-dimensional (3D) display of xenon-133 (^{133}Xe) gas SPECT data, and new analytical approaches by means of fractal analysis or the coefficient of variations of the pixel counts for Technegas SPECT data. The respiratory-gated image acquisition can partly eliminate problematic effects of the SPECT images obtained during non-breath-hold. The fusion image is available for routine clinical use, and provides complementary information on function and anatomy. The 3D displays of dynamic ^{133}Xe SPECT data are helpful for accurate perception of the anatomic extent and locations of impaired ventilation, and the assessment of the severity of ventilation abnormalities. The new analytical approaches facilitate the objective assessment of the degrees of ventilation abnormalities.

Key words: radionuclide imaging, lung ventilation, single photon emission computed tomography (SPECT), xenon-133 gas, Tc-99m-Technegas

INTRODUCTION

THE ROLE of pulmonary single photon emission computed tomography (SPECT) is now increasing in the field of respiratory nuclear medicine, since the evaluation of cross-sectional detail of pulmonary function coupled with morphologic computed tomography (CT) images is essential to understanding the pathophysiology of diseased lungs. Although, to date, technical and analytical methods for pulmonary ventilation SPECT studies have advanced step by step, there is still much room for improvements to facilitate more correct and perceptive interpretation and quantitation of SPECT data. For instance, a respiratory-gated SPECT acquisition can eliminate the problematic effects of the SPECT images obtained during nonbreath-hold. A fusion image of functional SPECT and anatomic CT images can provide the complementary information obtained from these images, and aids more accurate interpretation of regional ventilation abnormalities. A three-dimensional (3D) display of SPECT data facilitates the perception of the anatomic extent and locations of abnormally ventilated lung areas, and the assessment of the severity of ventilation abnormalities. This paper describes these recent advances in methods and analytical approaches for ventilation SPECT studies with technetium-99m (^{99m}Tc)-labeled Technegas and xenon-133 (^{133}Xe) gas.

Received May 31, 2002.

For reprint contact: Kazuyoshi Suga, M.D., Department of Radiology, Yamaguchi University School of Medicine, 1–1–1 Minamikogushi, Ube, Yamaguchi 755–8505, JAPAN.

(A) Technical Advances in SPECT Data Acquisition

(1) A respiratory-gated image acquisition for Tc-99m-Technegas SPECT

Because of the duration over which SPECT scans are acquired, breath-hold images cannot be obtained, resulting in problematic effects of respiratory movements of the lung. To solve this problem, in our institute, we use a respiratory gating system (AZ-733, Anzai Sogyo Co., Osaka, Japan) connected to a triple-headed SPECT unit (GCA 9300 A/PI, Toshiba Medical, Shibaura, Japan), where respiratory movement of the chest wall is monitored by a pressure-sensor placed on the body surface. Tc-99m-Technegas SPECT is one of the suitable

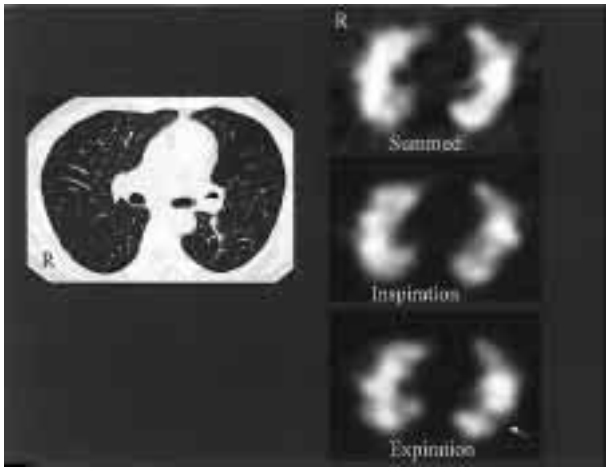

Fig. 1 Respiratory-gated ^{99m}Tc-Technegas SPECT study in a 41-year-old patient with diffuse panbronchiolitis. The chest CT image (*left*) at the lung level corresponding to the SPECT plane shows only focal tiny opacities along the peripheral bronchi. Although the conventional summed SPECT image shows heterogeneously-decreased Technegas distribution in both lungs, the ventilation heterogeneity and some of focal ventilation defects are more clearly seen on the matched inspiration and/or expiration phase SPECT images. A linear ventilation defect corresponding to the left major fissure is seen (*arrow*).

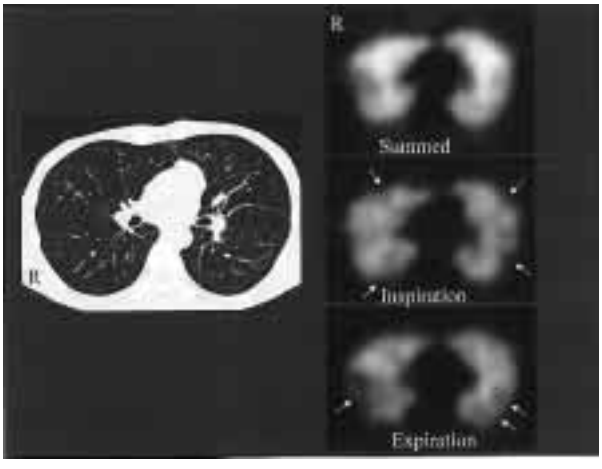

Fig. 2 Respiratory-gated Technegas SPECT study in a 56-year-old patient with acute bronchiolitis. The chest CT image at the lung level corresponding to the SPECT images shows only focal tiny opacities along the peripheral bronchi. Although the conventional summed SPECT image shows ventilation deficits mainly along the peripheral lung areas, these ventilation deficits are more discrete on the matched inspiration and expiration phase SPECT images (*arrows*).

examination methods for respiratory-gated image acquisition, because of the persistent radioactivity in the lungs (the biological half-life = 135 hour).[1–6] Although the lung radioactivity of the tracer is decreased to approximately one-eighth of that on the conventional summed SPECT images, the respiratory-gated, expiration-phase SPECT images appear to enhance the lesion-to-normal contrast especially in patients with relatively slight airway obstructive changes (Figs. 1, 2). This image is also expected to offer a more reliable fusion image with an anatomical CT image obtained similarly during breath-hold at the tidal inspiration level.

(2) Fusion of Tc-99m-Technegas SPECT and CT images
A fusion of functional SPECT and anatomical CT images gives the complementary information obtained from these images, and should facilitate accurate interpretations of SPECT data.[7,8] Recently we introduced a fusion image software with a fully automatic, multi-modality image registration algorithm to create a fusion image from ^{99m}Tc-Technegas SPECT and chest CT images for routine clinical practice. Technegas SPECT is performed under a respiratory gating in the three-headed SPECT unit (GCA 9300 A/PI, Toshiba Medical, Shibaura, Japan), and the inspiration phase SPECT images are registered with CT images obtained with a multi-detector raw scanner during a single breath hold at a tidal inspiration level. The automatic registration algorithm (ART in GMS 5500 A/DI, Toshiba Medical, Japan) has several attractive features: it is fully automatic and has the potential to be applied to a wide range of registration problems. The fusion is possible when the slice thickness is different from the chest CT scan. It can use multispectral CT images and multiple SPECT images simultaneously, hence using more information in the registration process.[9] The registration algorithm applies a rigid body transformation, and is based on the assumption that a segmentation of the chest CT image into connected components is also reflected in the SPECT image; the individual connected components are mostly composed of voxels from a single tissue type, and therefore the spatially corresponding SPECT voxels are expected to have similar values.[9] After segmentation of the body contours, the voxels inside the thorax are clustered into a set of connected components by using the k-means clustering algorithm (k = the number of desired classes), and the optimal registration parameters are automatically found by the method of coordinate descent and by minimizing the variance of the SPECT voxel values within each connected component.[9] As shown in Figures 3 and 4, the fusion is usually successful except for the cases with extensive defective areas of the radiotracer. When misregistration with a fully automatic registration occurs in these cases, the manual and visual registration is first done to obtain the pre-registration SPECT images grossly registered with CT images. Thereafter, the automatic registration algorithm usually allows the creation of more accurate fusion images. The registered SPECT and CT image greatly improves the interpretation of the SPECT findings. The locations of reduced Technegas distribution or abnormal hot spots can be easily and accurately seen. These images allow more accurate comparison between

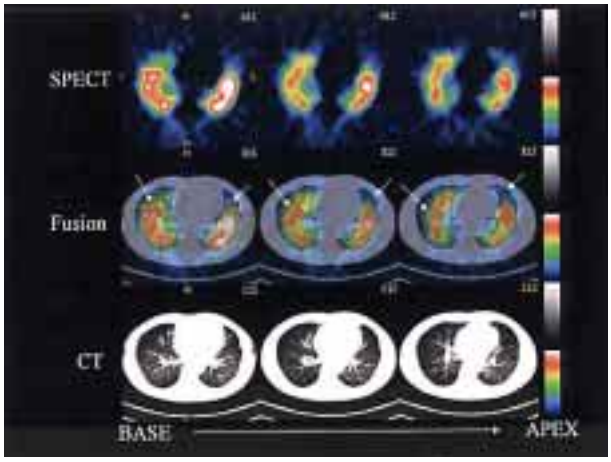

Fig. 3 The consecutive fusion images between the respiration-gated inspiration phase Technegas SPECT image and the tidal inspiration CT image, created by a fully automatic image registration algorithm, in a 41-year-old patient with diffuse panbronchiolitis. The fusion images show heterogeneously-reduced Technegas distribution in both lungs, especially corresponding to the relatively low attenuation lung areas on chest CT scan (*arrows*).

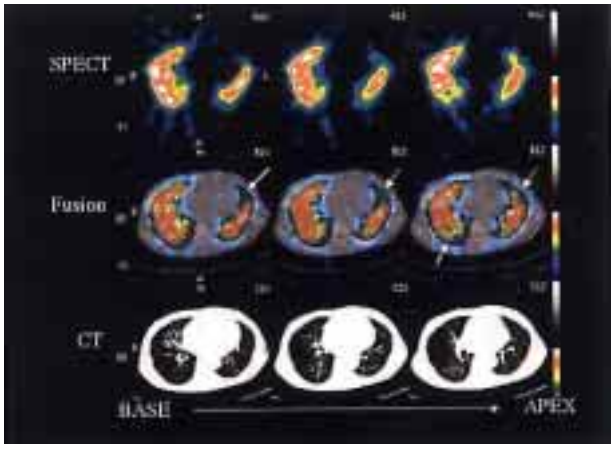

Fig. 4 The consecutive fusion images between the respiration-gated inspiration phase Technegas SPECT image and the tidal inspiration CT image, created by a fully automatic image registration algorithm, in a 48-year-old woman recovered from acute respiratory distress syndrome. The fusion images clearly show that Technegas distribution is mainly reduced in the lung areas with still remained focal infiltrate along the bronchi on CT images (*arrows*).

function and anatomy in various lung pathologies, and allow more definitive diagnosis than can be obtained by simple visual comparison of the non-registered images (Fig. 3). The additional fusion images with ^{99m}Tc -macro-aggregated human serum albumin (MAA) perfusion SPECT permit more accurate assessment of the presence or absence of ventilation and perfusion mismatches in patients with suspected pulmonary embolism.

A major obstacle to body image registration arises from the fact that the thorax cannot be considered a rigid body. CT scans are obtained during a single breath-hold, whereas the SPECT images are obtained during quiet respiration. Such issues as respiratory and cardiac motion and the deformable nature of the human torso must be considered to fully address the registration problems.[7] Nevertheless, respiratory diaphragmatic excursion during the tidal breathing is usually only slightly greater than the spatial resolution of the SPECT camera and creates little additional misregistration on fused images; the diaphragm dome usually moves only 1 to 2 cm in healthy supine adults during tidal breathing.[10] Further, the diaphragmatic excursion may be even less in patients with underlying chronic obstructive lung diseases or with poorly compliant, fibrotic lungs.[10] In extreme cases, where SPECT images bear little resemblance to the underlying anatomical CT images because of marked perfusion or ventilation defects, the use of transmission images may be an alternative to be considered.[8,10]

(3) Dynamic ^{133}Xe SPECT

Dynamic ^{133}Xe SPECT is a useful tool for accurately assessing the extent and location of air trapping in lung regions, without superimposition of lung tissues,[11,12] and is superior to planar imaging study in the sensitive detection of ^{133}Xe retention in a patient's lungs. Dynamic ^{133}Xe SPECT for an equilibrium (EQ) and subsequent washout (WO) phase after inhalation of ^{133}Xe gas (concentration; 60–72 MBq/liter) is performed in a continuous repetitive rotating acquisition mode with a multi-detector SPECT system.[11,12] To eliminate the settling time between projections and acquisition of multiple temporal samples of data, each detector is continuously and repeatedly rotated in the clockwise and counterclockwise directions across the same projection arc (Fig. 5). Averaged projection data at the same angle in both directional rotations is used for reconstructing a single SPECT image, so that change in ^{133}Xe activity in the lungs during the acquisition time is averaged. Dynamic ^{133}Xe SPECT is an intrinsically quantitative technique which permits the assessment of regional lung ventilation. As in the planar study, regional ventilation can be quantified by calculating ^{133}Xe half clearance time (T1/2) on a regional basis. There is a good correlation in T1/2 between ^{133}Xe SPECT and planar studies.[11] Lung perfusion SPECT study with ^{99m}Tc-MAA is usually coupled with ^{133}Xe SPECT study.

Dynamic ^{133}Xe SPECT allows the perception of cross sectional lung pathophysiologies in various lung diseases with airway obstruction.[11–14] For instance, in patients with a long-term smoking history and relatively advanced emphysema, dynamic ^{133}Xe SPECT often demonstrates significantly faster ^{133}Xe clearance in the peripheral lung than in the central lung, accompanied with a well-known,

stripe sign on perfusion SPECT images (Fig. 6).[14] The majority of these lung zones show central-dominant low attenuation lung area (LAA) distributions on chest CT images. This relative preservation of peripheral lung function may be a characteristic feature in smoking-related pulmonary emphysema, and this difference between peripheral and central lungs in the susceptibility of emphysematous changes can be partly explained by structural differences in pulmonary lobules and by instability of interlobular septa in the central lung.[14]

Pulmonary dynamic densitometry acquired by spiral CT scanning or by an ultrafast electron-beam CT scanning may allow quantitative estimation of the rapid process of lung density change during respiration, and has been used for detecting ventilation abnormalities.[15] But, because lung density on a CT scan is determined not only by air volume but also by lung tissue and blood volume, it is necessary to assess whether lung density change abnormalities on dynamic CT densitometry can correctly reflect regional aeration abnormalities. Our previous comparative study with dynamic ^{133}Xe SPECT indicates that dynamic densitometry acquired by spiral CT scan may be an acceptable approach to detect ventilation abnormalities associated with obstructive airways disorder, as the regional maximal amplitude in lung density change correlated inversely with ^{133}Xe clearance-time in regional lungs (Fig. 7).[15]

(B) Analytical Advances in Interpretation of SPECT Data

(1) 3D surface-rendering display of ^{133}Xe dynamic SPECT

Interpretation of transaxial images of ^{133}Xe dynamic SPECT study, however, may be often difficult, since the viewer must deal with many washout sequences which show an elimination of ^{133}Xe activity and often lack anatomic detail. To facilitate the interpretation of the data and perception of the anatomic location and extent of ^{133}Xe retention sites, we have developed a single 3D fusion image by using well-established surface-rendering techniques.[15] This 3D image is created from two different time-course image sets of 3D images of the equilibrium (EQ) and 3-min washout (WO) images, where the 3D EQ image delineates the lung contours or volumes, and the 3-min washout image represents ^{133}Xe retention sites (Fig. 8). Volumetric extent of ^{133}Xe retention (air trapping) in regional lung can be quantified by the ^{133}Xe retention index, defined as the ratio (%) of the total numbers of pixels in the segmented 3-min WO image data (volume of areas with ^{133}Xe retention) to those of EQ data (lung volume).[15] Although almost all of the retention sites are seen on the multislice 3-min washout images, the spatial relationships and extent of the retention are more easily and accurately comprehended on this 3D display. This topographic 3D display simplifies the interpretation of multislice data of ^{133}Xe SPECT and facilitates the perception of anatomic distributions of ^{133}Xe retention with geometric realism.[16]

The interaction between impaired respiratory mechanics and abnormal lung ventilation in patients with obstruc-

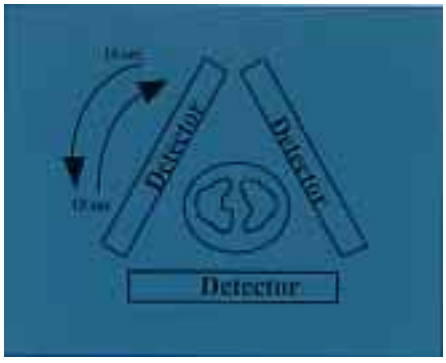

Fig. 5 Schematic representation of ^{133}Xe dynamic SPECT examination using triple-headed detector SPECT unit. To eliminate the settling time between projections and acquisition of multiple temporal samples of data, each detector is continuously and repeatedly rotated in the clockwise and counterclockwise directions across the same projection arc. Averaged projection data at the same angle in both directional rotations is used for reconstructing a single SPECT image, so that the elimination of ^{133}Xe activity in the lungs during the acquisition time of 30 sec is averaged.

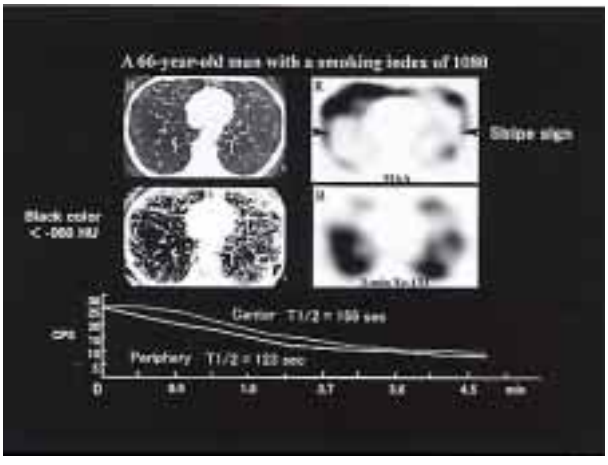

Fig. 6 A 66-year-old man with a smoking index of 1080. A chest CT scan (*top, left*) shows emphysematous and/or bullous changes predominantly in the central lungs. The density mask CT image (middle, left), which specifically visualizes the low attenuation lung area (LAA) with lung attenuation values of –960 Hounsfield units (HU) as a monotonous black color, shows central-dominant LAA distributions. ^{99m}Tc-MAA SPECT (*top, right*) shows periphery-dominant perfusion with central perfusion defects in both lungs. A ^{133}Xe SPECT image 3 min after initiation of washout (*middle, right*) shows ^{133}Xe retention mainly in the central lung area. The time-activity curves in the right lung (*bottom*) show a more prolonged T1/2 in the central lung area than in the peripheral lung area.

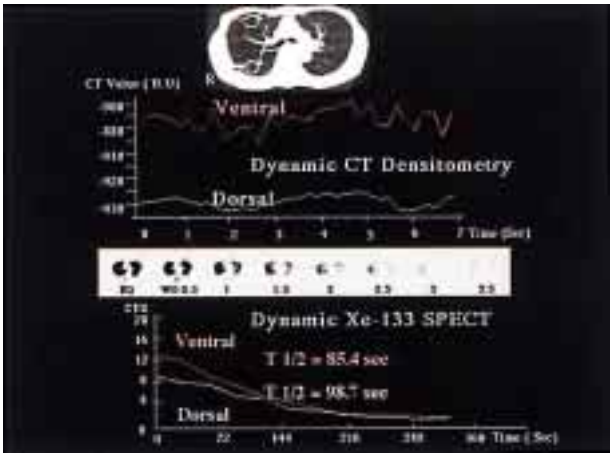

Fig. 7 Dynamic expiratory spiral CT with ROIs at the middle lung zone, and pulmonary densitometry (PDD) in a 57-year-old man with pulmonary emphysema. A chest CT image (*top*) shows patchy hyperlucency diffusely in both lungs. The PDD (the 2nd line) shows flattened and irregular curves in both the right ventral and dorsal lungs. ^{133}Xe SPECT images (3rd line) shows abnormal ^{133}Xe retention in both lungs. ^{133}Xe clearance curves (*bottom*) shows more prolonged ^{133}Xe clearance in the right lung area with more reduced respiratory changes in CT attenuation. H.U. = Hounsfield units, CPS = counts per second.

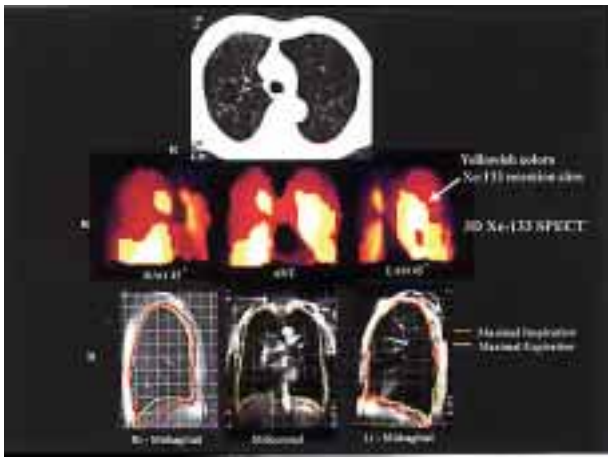

Fig. 8 Assessment of the interaction between ^{133}Xe retention assessed on ^{133}Xe dynamic SPECT and respiratory mechanics assessed by dynamic breathing magnetic resonance (MR) imaging in a 79-year-old man with generalized emphysema. A chest CT image (*top*) shows marked emphysematous changes in both lungs. A three-dimensional surface-rendering ^{133}Xe SPECT displays (*middle*) show greater ^{133}Xe retention (*yellowish colors*) in the left lung (*arrow*) than in the right lung. Fusion MR displays (*bottom*) of the maximal inspiration and expiration MR images show reduced diaphragm/chest wall motions especially in the left thorax with greater ^{133}Xe retention. The ^{133}Xe SPECT displays are created from two different time-course image sets of 3D images of the equilibrium and 3-min washout images, where the 3D EQ image delineates the lung contours or volumes, and the 3-min washout image represents ^{133}Xe retention sites (*yellowish colors*).

tive lung disease can be evaluated by the comparison between 3D ^{133}Xe dynamic SPECT images and fast magnetic resonance (MR) imaging which directly visualizes regional respiratory diaphragm (D)/chest wall (CW) motions. This analysis appears fundamental to systematic understanding of pathophysiologic compromises in these patients. Our preliminary comparison of regional respiratory mechanics with lung ventilation assessed by these techniques has demonstrated a close interaction between these impairments in patients with pulmonary emphysema[17] (Fig. 8). These patients showed reduced, irregular or asynchronous motions in the thorax with greater ^{133}Xe retention, with significant decreases in the maximal amplitude of D/CW movement. There were also significant correlations between D/CW motions and $\%FEV_1$, and the ^{133}Xe retention index in each thorax.[17] Furthermore, the removal of ^{133}Xe retention sites by lung volume reduction surgery (LVRS) effectively and regionally improved D/CW movement.

(2) 3D volume-rendering functional images of ^{133}Xe dynamic SPECT

The surface-rendering 3D image mentioned above, however, included only the 3-min washout (WO) data to assess ventilation abnormality, and the image feature is heavily dependent on the thresholds chosen. To fully interpret the dynamic ^{133}Xe SPECT study and to address the deficiencies in the surface-rendering 3D display described above, we have recently developed a volume-rendering 3D image to represent all data from ^{133}Xe WO process in voxel-by-voxel order in a more useful form as a functional image of lung ventilation (Figs. 9, 10). In these, various ventilation parameters are estimated by applying a height-over-area method to the washout curves in voxel-by-voxel order. The time-activity curves for each pixel in the transaxial slices are fit to a mono-exponential function to determine the mean transit time (MTT) and ventilation rate (λ = 1/MTT, time constant).[18] In addition to these parameters, lung volume (EQ data) and ^{133}Xe retention (3-min WO data) are reconstructed into realistic and quantitatively accurate 3D images, by a volume-rendering technique. The cross-sectional functional images are also simultaneously displayed at any selected, orthogonal lung planes (Figs. 9, 10). These functional 3D images permit full interpretation of a ^{133}Xe SPECT study, and contribute to better perception of regional ventilation impairment.

A ^{133}Xe dynamic SPECT study, which effectively detects poorly ventilated lung areas with air trapping, is useful and logical for selecting the target lung tissue for thoracoscopic lung volume reduction surgery (LVRS), because multiple resections of the most overdistended, poorly ventilated lung tissues with air trapping is the principle of LVRS.[19,20–23] ^{133}Xe SPECT makes it

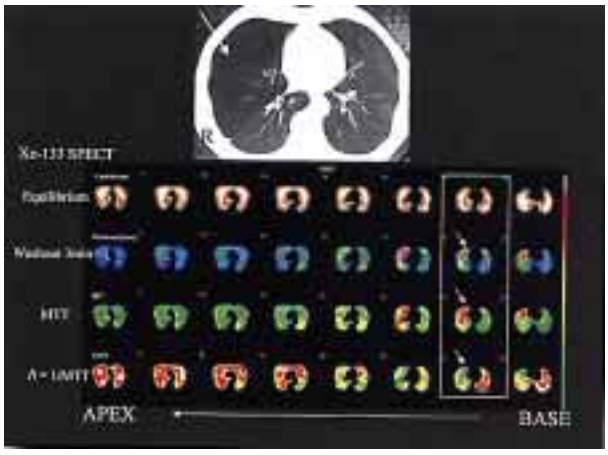

A

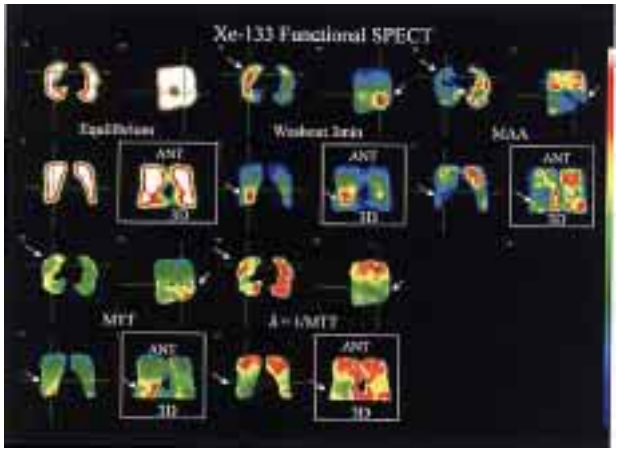

B

Fig. 9 The 3D functional ^{133}Xe SPECT displays in a 69-year-old patient with a large bullous change in the right lung. (A) A chest CT image shows marked bullous change in the right lung. The consecutive cross-sectional functional images of the equilibrium, 3-min washout, mean transit time (MTT), and ventilation rate (λ = 1/MTT) SPECT images show that ventilation is markedly impaired corresponding to the bullous area, with severe ^{133}Xe retention on 3-min washout images, prolonged MTT and decreased ventilation rate (*white square; arrows*). (B) The volume-rendering 3D functional images, reconstructed from the above consecutive cross-sectional functional images, and the 3D ^{99m}Tc-MAA perfusion SPECT images show that the right bullous area has the worst lung function (*arrows*). The cross-sectional functional images at the selected orthogonal lung planes are also simultaneously displayed, representing the locations with the worst lung function in each cross-sectional plane (*arrows*).

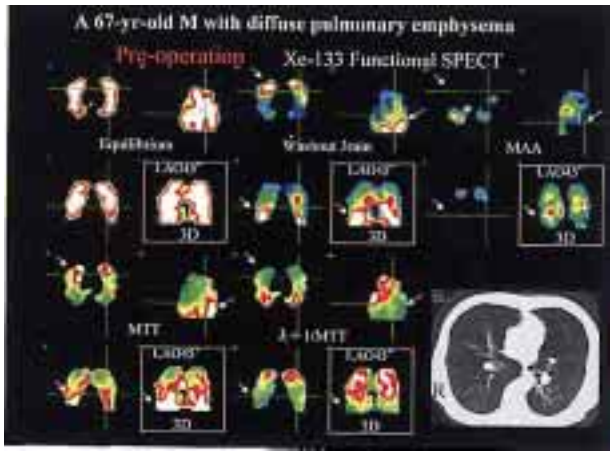

A

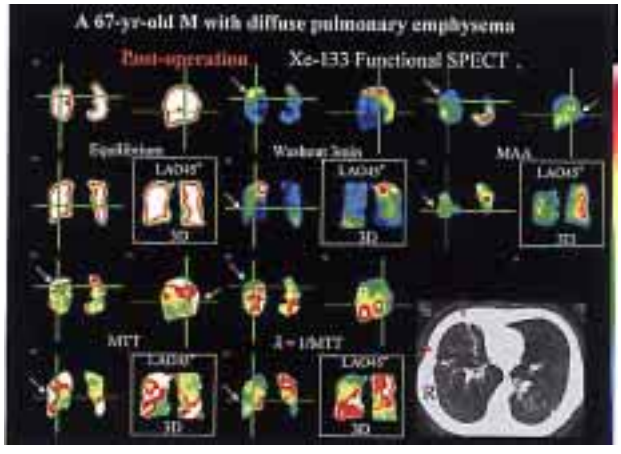

B

Fig. 10 The volume-rendering 3D functional ^{133}Xe SPECT displays in a 67-year-old patient with diffuse pulmonary emphysema, who underwent thoracoscopic lung volume reduction surgery (LVRS). (A) Although the pre-operative chest CT image (*right below*) shows diffuse emphysematous changes, the 3D functional SPECT images of 3-min washout, mean transit time (MTT), and ventilation rate (λ = 1/MTT) show the lung areas with the mostly impaired lung function (*white square; arrows*). (B) After resection the right ventral portion with the mostly impaired lung function as seen in the chest CT scan (*right below: red arrows*), the post-operative 3D functional SPECT images show the improvement of lung ventilation at the resected lung area, accompanied with improved perfusion (*arrows*).

possible to efficiently and adequately localize the most affected areas even in LVRS-candidates with widely or homogeneously spreading nonbullous emphysematous tissues on chest CT scan. The topographic 3D displays of ^{133}Xe SPECT mentioned here appear to be very useful for selecting resection targets for LVRS, and for evaluating the treatment effects on regional ventilation.[19,20]

(3) New analytical approaches for Technegas SPECT

New quantitative approaches by means of a fractal analysis[24] or the coefficient of variation (CV) of the pixel counts[25] have recently been introduced for objective evaluation of inhomogeneity in ventilation SPECT with

Technegas. In the fractal analysis, the number of pixels delineated with several adequate cut-off levels of maximal pixel intensity are measured to derive the fractal dimension and to evaluate the heterogeneity of radioaerosol distribution.[24] The analysis of the CV within and between small lung elements in Technegas ventilation SPECT and parametric images of micro-level CV values appears useful to assess and visualize the localization and severity of regional inhomogeneity.[25] Although Technegas distribution may not reflect ventilation distribution perfectly because of its aerosol properties in some cases, these new analytical approaches can provide information on the overall ventilation inhomogeneity, and represent one step in the development of quantification of the SPECT technique with the aim of achieving functional tomography.

In conclusion, this paper described the recent advances in the methodological and analytical approaches for pulmonary ventilation SPECT studies with Technegas and ^{133}Xe gas. These advances will contribute to provide more accurate and perceptive interpretation of SPECT data, and will enhance the role of SPECT studies in the field of respiratory medicine.

ACKNOWLEDGMENTS

Part of ^{133}Xe dynamic SPECT study was supported by a Grant for Scientific Research (08671033) from the Japanese Ministry of Education, Science, Sports & Culture.

REFERENCES

1. Fujita J, Takahashi K, Satoh K, Okada H, Momoi A, Yamadori I, et al. Tc-99m Technegas scintigraphy to evaluate the lung ventilation in patients with oral corticosteroid-dependent bronchial asthma. *Ann Nucl Med* 1999; 13: 247–251.
2. Satoh K, Takahashi K, Sasaki M, Kobayashi T, Honjo N, Ohkawa M, et al. Comparison of Tc-99m-Technegas SPECT with Xe-133 dynamic SPECT in pulmonary emphysema. *Ann Nucl Med* 1997; 11: 201–206.
3. Castellani M, Vanoli M, Cali G, et al. Ventilation-perfusion lung scan for the detection of pulmonary involvement in Takayasu's arteritis. *Eur J Nucl Med* 2001; 28: 1801–1805.
4. Imai T, Sasaki Y, Shinkai T, Ohishi H, Nezu K, Nishimoto Y, et al. Clinical evaluation of Tc-99m-Technegas SPECT in thoracoscopic lung volume reduction surgery in patients with pulmonary emphysema. *Ann Nucl Med* 2000; 14: 263–269.
5. Howarth DM, Lau L, Thomas PA, Allen LW. Tc-99m Technegas ventilation and perfusion lung scintigraphy for the diagnosis of pulmonary embolus. *J Nucl Med* 1999; 40: 579–584.
6. Hartmann IJC, Hagen PJ, Stokkel MP, et al. Technegas versus Kr-81m ventilation-perfusion scintigraphy; a comparative study in patients with suspected acute pulmonary embolism. *J Nucl Med* 2001; 42: 393–400.
7. Aquino SL, Asmuth JC, Moore R, Weise SB, Fischman AJ. Improved image interpretation with registered thoracic CT and positron emission tomography data sets. *AJR* 2002; 178: 939–944.
8. Dey D, Slomka PJ, Hahn LJ, Kloiber R. Automatic three-dimensional multimodality registration using radionuclide transmission CT attenuation maps: a phantom study. *J Nucl Med* 1999; 40: 448–455.
9. Ardekani BA, Braun M, Hutton BF, Kanno I, Iida H. A fully automatic multimodality image registration algorithm. *J Comput Assist Tomogr* 1995; 19: 615–623.
10. Ketai L, Hartshorne M. Potential of computed tomography—SPECT and computed tomography—coincidence fusion images of the chest. *Clin Nucl Med* 2001; 26: 433–441.
11. Suga K, Nishigauchi K, Kume N, et al. Dynamic pulmonary SPECT of xenon-133 gas washout. *J Nucl Med* 1996; 37: 807–814.
12. Suga K, Hara A, Matsumoto T, et al. Intralobar broncho-pulmonary sequestration: dynamic xenon-133 SPECT evidence of air trapping. *BJR* 2001; 74: in press.
13. Suga K, Shimizu K, Kume N, et al. Evaluation of abnormal regional ventilation in patients with lung cancer using three-dimensional display of dynamic xenon-133 SPECT. *Nucl Med Commun* 1998; 19: 593–598.
14. Suga K, Kume N, Matsunaga N, et al. Relative preservation of peripheral lung function in smoking-related pulmonary emphysema: Assessment with Tc-99m MAA perfusion and dynanic Xe-133 SPECT. *Eur J Nucl Med* 2000; 27: 800–806.
15. Suga K, Nishigauchi K, Kume N, et al. Pulmonary dynamic densitometry acquired by spiral CT to detect ventilation abnormalities in obstructive airway disorders: comparison with dynamic Xe-133 SPECT. *Radiology* 1997; 202: 855–862.
16. Suga K, Kume N, Nishigauchi K, et al. Three-dimensional surface display of dynamic pulmonary xenon-133 SPECT in patients with obstructive lung disease. *J Nucl Med* 1998; 39: 889–893.
17. Suga K, Tsukuda T, Awaya H, et al. Interactions of regional respiratory mechanics and pulmonary ventilatory impairment in pulmonary emphysema: Assessment with dynamic MRI and Xenon-133 SPECT. *Chest* 2000; 117: 1646–1655.
18. Dollfuss RE, Milic-Emili J, Bates DV. Regional ventilation of the lung studied with boluses of Xenon-133. *Respir Physiol* 1967; 2: 234–246.
19. Suga K, Nishigauchi K, Matsunaga N, et al. Preliminary application of dynamic pulmonary xenon-133 single-photon emission tomography in the evaluation of patients with pulmonary emphysema for thoracoscopic lung volume reduction surgery. *Eur J Nucl Med* 1998; 25: 410–416.
20. Suga K, Nishigauchi K, Matsunaga N, et al. Radionuclide imaging in emphysema after lung volume reduction surgery. *Clin Nucl Med* 1997; 22: 683–686.
21. Hoppin FG. Theoretical basis for improvement following reduction pneumoplasty in emphysema. *Am J Respir Crit Care Med* 1997; 155: 520–525.
22. Naunheim KS, Keller CA, Krucylak PE, et al. Unilateral video-assisted thoracic surgical lung reduction. *Ann Thorac Surg* 1996; 61: 1092–1098.
23. Martinez FJ, Montes MM, Whyte RI, et al. Lung-volume reduction improves dyspnea, dynamic hyperinflation, and respiratory muscle function. *Am J Respir Crit Care Med*

1997; 155: 1984–1990.
24. Nagao M, Murase K, Ichiki T, et al. Quantitative analysis of technegas SPECT: evaluation of regional severity of emphysema. *J Nucl Med* 2000; 41: 590–595.
25. Xu J, Moonen M, Johansson A, et al. Quantitative analysis of inhomogeneity in ventilation SPET. *Eur J Nucl Med* 2001; 28: 1795–1800.